scientific reports

Check for updates

OPEN

Toxoplasma GRA16 attenuates Tau hyperphosphorylation and enhances autophagy in thrombin-treated HT-22 hippocampal neuronal cells

Seung-Hwan Seo[1,2], Do-Won Ham[2], Ji-Eun Lee[2] & Eun-Hee Shin[1,2,3]✉

This study investigated whether *Toxoplasma gondii*-derived dense granule protein 16 (GRA16) modulates tau protein to attenuate tau hyperphosphorylation and promotes autophagy to facilitate the removal of tau aggregates. HT-22 murine hippocampal neuronal cells were treated with thrombin to induce rapid hyperphosphorylations and tau aggregation. Thrombin increased hyperphosphorylated tau protein levels and activated NF-κB, contributing to tau pathology and neuroinflammation. NF-κB activation increased apolipoprotein E (APOE) expression and decreased forkhead box O3A (FOXO3A) expression, a factor involved in autophagy regulation, consequently limiting the expression of autophagy-related genes directly regulated by FOXO3A. Meanwhile, in GRA16-transfected HT-22 cells treated with thrombin, GRA16 upregulated proteins involved in tau dephosphorylation but downregulated protein involved in tau phosphorylation. Moreover, GRA16 inhibited thrombin-induced NF-κB activation and increased FOXO3A levels, thereby enhancing the expression of autophagy-related genes, including those directly regulated by FOXO3A. GRA16 enhanced intracellular autophagic flux and inhibited tau hyperphosphorylations in thrombin-treated HT-22 cells, as evidenced by increased autophagic fluorescence and significant reductions in phosphorylated tau protein levels and fluorescence intensity. These findings suggest that GRA16 possesses therapeutic potential in tauopathies by enhancing tau dephosphorylation and autophagy-mediated tau clearance, establishing a conceptual foundation for developing new therapeutic approaches targeting tau pathology.

Keywords Autophagy, Dense granule protein 16, Hippocampal neuronal cell, Hyperphosphorylated Tau, Tauopathy, *Toxoplasma gondii*

Alzheimer's disease (AD) remains the leading cause of dementia, accounting for 60–80% of cases among the elderly population[1]. This condition is characterized by a progressive and irreversible decline in cognition, behavior, and responsiveness to the environment, with affected individuals presenting with various symptoms, such as memory loss, impaired learning, and difficulties with cognition and language[1,2]. The development of AD can be attributed to two main pathological features: extracellular neuritic plaques resulting from β-amyloid (Aβ) accumulation and intracellular neurofibrillary tangles (NFTs) composed of hyperphosphorylated tau protein[3]. In particular, misfolded, hyperphosphorylated tau proteins have been considered a pivotal factor in the pathogenesis of AD and other tauopathies. Consequently, inhibiting the aggregation of hyperphosphorylated tau proteins could be a promising strategy for the discovery and development of therapeutics against AD[3,4].

Tau pathologies tend to directly promote neuroinflammation[5]. Tau is mainly localized to neurons and, to a lesser extent, is also expressed in oligodendrocytes and astrocytes. Its primary function is its role in the assembly and stabilization of neuronal microtubules[3]. However, the neurofibrillary lesions observed in brain tauopathies, including NFTs in AD, are characterized by highly-ordered aggregations of hyperphosphorylated tau filaments[6]. In 2003, Suo et al. demonstrated that treatment with nanomolar concentrations of thrombin can induce rapid hyperphosphorylation and aggregation of tau in hippocampal neurons[7]. Thrombin, a pleiotropic

[1]Institute of Endemic Diseases, Medical Research Center, Seoul National University, Seoul, Korea. [2]Department of Tropical Medicine and Parasitology, Seoul National University College of Medicine, Seoul, Korea. [3]Seoul National University Bundang Hospital, Seongnam, Korea. ✉email: ehshin@snu.ac.kr

enzyme and serine protease involved in blood coagulation, can exert pathogenic effects on neurons[8]. Under pathological conditions, thrombin levels are usually elevated. Alternatively, thrombin may abnormally infiltrate neuronal tissue. Thrombin activates protease-activated receptors (PARs), leading to tau aggregation and hippocampal degeneration[9]. These findings pathogenetically link thrombin to neuroinflammation, including brain tauopathies, associated with cerebrovascular damage, and suggest that thrombin can be employed in in vitro cell models to investigate these tauopathies.

Autophagy is a lysosome-dependent, evolutionarily conserved cellular process in eukaryotes. This process has been closely associated with the regulation of protein metabolism considering that it enables the degradation and recycling of damaged organelles and misfolded proteins to maintain protein homeostasis. Increasing evidence suggests that autophagy is involved in the regulation of AD pathogenesis[10]. A reduction in autophagy can cause neurodegeneration, whereas its stimulation can protect against some proteinopathies. Silva et al. (2020) used neurons from patients with AD to demonstrate that tau reduction in these cells requires autophagy through the sequestration of the cells into phagolysosomes[11]. Notably, tau clearance in neurons was predominantly achieved through the inhibition of mammalian target of rapamycin (mTOR) and mammalian target of rapamycin complex 1 (mTORC1). This is induced by mTOR inhibitors that promote autophagy-mediated tau clearance[11]. Therefore, in AD, especially with tau pathology, autophagy evidently serves as an essential defense of brain cells through its degradation of NFTs formed by hyperphosphorylated tau protein. Studies have also highlighted the importance of activating autophagy in a neuroinflammatory environment[11–13].

Apolipoprotein E (APOE) plays a crucial role in the pathogenesis of AD. Notably, three predominant APOE variants exist in humans, namely ε2, ε3, and ε4[14]. Among these variants, APOE ε4 has been strongly associated with an increased risk of AD. Reports have also shown that polymorphisms in the APOE promoter were correlated with increased AD susceptibility. Aside from humans, mouse models of APOE expression have long been used to study the mechanisms underlying the pathogenesis of AD[15]. In the context of AD pathogenesis, Sohn et al. (2021) demonstrated that APOE variants increase the accumulation of hyperphosphorylated tau by impairing autophagy through the repression of forkhead box O3A (FOXO3A)[16], a transcription factor that plays a crucial role in regulating various cellular processes, particularly autophagy. More specifically, FOXO3A activates autophagy by upregulating the expression of autophagy-related genes[16,17]. Numerous studies suggest that the activation of FOXO3A and subsequent enhancement of autophagy may serve as a neuroprotective mechanism against the accumulation of hyperphosphorylated tau and other toxic proteins associated with AD[17].

Dense granule protein 16 (GRA16), which is secreted by the parasitic protozoan *Toxoplasma gondii (T. gondii)*, has been found to play an important role in modulating the host cell environment to favor *T. gondii* survival and replication[18]. Once secreted, GRA16 is transported across the parasitophorous vacuole into the cytoplasm and nucleus of the host cell[18]. GRA16 directly interacts with B55 regulatory subunit of protein phosphatase 2 A (PP2A-B55) and ubiquitin-specific protease 7 (USP7) or indirectly with phosphatase and tensin homolog (PTEN) within host cells to regulate key signaling pathways associated with the cell cycle, apoptosis, and immune responses[18–20]. By leveraging the functional properties of GRA16, our previous studies demonstrated that GRA16 upregulates the critical tumor suppressors PP2A-B55 and PTEN in cancer cells located in the liver, lungs, and colon and downregulates nuclear factor kappa B (NF-κB), a transcriptional factor that promotes cell cycle progression, proliferation, invasion, and metastasis of cancer cells[21–23].

With this background, the current study aimed to investigate the following. First, AD was associated with hyperphosphorylated tau, which directly promotes the progression of neuroinflammation. Second, autophagy functions as an essential defense mechanism for degrading NFTs formed by hyperphosphorylated tau in brain cells. Third, during the pathogenesis of AD, the upregulated APOE suppresses FOXO3A, a key regulator of the transcriptional expression of autophagy-related genes, thereby constraining autophagy activation. Therefore, we investigated whether GRA16 reduces the hyperphosphorylation and aggregation of tau protein and promotes autophagy by upregulating FOXO3A through the suppression of APOE in thrombin-induced neuroinflammatory hippocampal neuronal cells.

Importantly, this study might foster a more profound understanding of the molecular processes involved in tau hyperphosphorylation and aggregation that drive neuroinflammation, as well as the autophagy mechanisms that counteract them. Furthermore, our results potentially provide a conceptual foundation for developing new therapeutic approaches that utilize GRA16 as a novel tauopathy downregulator and autophagy enhancer.

Methods

Cell culture

Mouse hippocampal neuronal cell line (HT-22) was obtained from the Korean Cell Line Bank (Seoul, Korea). The retroviral packaging cell line (Platinum-A) was purchased from Cell Biolabs (San Diego, CA, USA). HT-22 and Platinum-A cells were maintained in Dulbecco's Modified Eagle Medium (DMEM) (Welgene, Gyeongsan, Korea) supplemented with 10% fetal bovine serum (FBS) (Welgene) and 1% antibiotic–antimycotic (AA) (Welgene). HT-22 cells were differentiated in neurobasal medium (Thermo Fisher Scientific, Waltham, MA, USA) containing 2 mM L-glutamine (Thermo Fisher Scientific) and 1 × N-2 supplement (Thermo Fisher Scientific) for 24 h prior to use.

Cell transduction

To produce HT-22 cells stably expressing the GRA16 protein, we prepared a retrovirus transfer plasmid (*pBABE-HAII-GRA16*) containing the *gra16* gene constructed in a previous study[23]. Platinum-A cells were seeded into 6-well plates at 5×10^5 cells per well 24 h before transfection. Thereafter, 2.5 μg of DNA constructs were transfected into each well using Lipofectamine 3000 kit (Thermo Fisher Scientific) and Opti-Minimal Essential Medium (Opti-MEM) (Thermo Fisher Scientific). Afterward, 1.5 μg of *pBABE-HAII-GRA16*, 0.75 μg of *pCMV-Gag-Pol* (Retrovirus packaging plasmid), and 0.25 μg of *pMD2.G* (Retrovirus envelop plasmid) were mixed

with 5 µL of P3000 reagent and 5 µL of Lipofectamine 3000 reagent in 250 µL of Opti-MEM (Thermo Fisher Scientific). After 15 min of incubation at room temperature, the mixture was added to the Platinum-A cells. After 48 h of transfection, the cell culture medium was harvested, centrifuged for 5 min with 1,000 × *g* and filtered using a 0.45-µm filter. The supernatant was frozen using liquid nitrogen and stored at − 80 °C before using. For viral transduction, HT-22 cells were seeded into 6-well plates at 5×10^5 cells per well. After 24 h, the viral supernatant was distributed to each well with 8 µg of polybrene (Santa Cruz Biotechnology, Santa Cruz, CA, USA) and incubated for 48 h. GRA16 protein-expressing HT-22 cells were selected using a fresh DMEM medium supplemented with 10% FBS and 1% AA with 2 µg/mL of puromycin (Santa Cruz Biotechnology).

RNA extraction and real-time quantitative polymerase chain reaction (qPCR)

Total RNA from the cells was extracted using the HiGene™ Total RNA Prep Kit (BioFact, Daejeon, Korea). Using a Reverse-Transcription Premix (Elpis Biotech, Daejeon, Korea), 1 µg of the RNA was incubated at 70 °C for 5 min and reverse transcribed to cDNA using the following conditions: 42 °C for 1 h, then 94 °C for 5 min, in a 20 µL of reaction volume. Subsequently, real-time qPCR was performed using 20 µL of reaction mixture comprising 1 µL of cDNA, 10 pmol of primers, and 10 µL of TOPreal™ qPCR 2X PreMIX (SYBR Green with low ROX) (Enzynomics, Daejeon, Korea). Amplification reactions were performed at 95 °C for 15 min, followed by 40 cycles of 95 °C for 20 s, 59 °C for 20 s, and 72 °C for 30 s. SYBR Green fluorescent signals were assessed using iQ™5 optical system software (Bio-Rad Laboratories, Hercules, CA, USA). The relative expression of the target gene was compared to that of the control group after normalizing it to the Ct value of *GAPDH*. The primer sequences of the target genes were obtained from OriGene™ Technologies (Rockville, MD, USA). All primer sequences are listed in Table 1.

Western blot analysis

Total proteins from HT-22 cells were extracted using M-PER™ Mammalian Protein Extraction Reagent (Thermo Fisher Scientific). Proteins were quantified using Pierce™ BCA Protein Assay Kit (Thermo Fisher Scientific). A total of 30 µg of proteins per mini-gel well was separated using 12% SDS-PAGE and transferred onto polyvinylidene fluoride membranes at 100 V for 1 h at 4 °C using the Mini Trans-Blot® Electrophoretic Transfer Cell (Bio-Rad Laboratories) instrument. The transferred membranes were blocked in 5% bovine serum albumin (BSA) in TBS-T (TBS with 0.1% Tween-20) for 1.5 h at room temperature. The blocked membranes were incubated with primary antibodies for 16 h at 4 °C. Thereafter, the membranes were washed three times with TBS-T and incubated with horseradish peroxidase-conjugated secondary antibodies for 1 h at room temperature. Target proteins on the membrane were visualized using Pierce™ ECL western Blotting Substrate (Thermo Fisher Scientific). Images were captured using Amersham Imager 680 (GE healthcare, Chicago, IL, USA), and the signal intensities were calculated using ImageJ (free software provided by the National Institutes of Health). The relative expression of the target protein was normalized to the density value of β-actin and compared to that in the control group. All antibodies are listed in Table 2.

Immunofluorescence

HT-22 cells were fixed with 4% paraformaldehyde solution for 10 min at room temperature. After washing with PBS (pH 7.5), the cells were treated for 15 min at room temperature with a permeabilization solution (PBS with 0.2% Triton X-100), incubated with a blocking buffer (PBS with 0.1% Tween-20 containing 1% BSA and 22.52 mg/mL glycine) for 1 h at room temperature, washed with PBS-T (TBS with 0.1% Tween-20) buffer, and then stained with antiphospho-Tau antibody (Ser202/Thr205, AT8) (Invitrogen) for 16 h at 4 °C. After washing with PBS-T, the cells were stained with donkey antimouse IgG (H + L)-Alexa Fluor 594 antibody (Invitrogen) as a secondary antibody for 1 h at room temperature in the dark. Thereafter, the cells were washed with PBS-T and stained with Hoechst33342 (Sigma–Aldrich, St. Louis, MO, USA) diluted in PBS (5 µg/mL) for 5 min at room temperature in the dark. After another wash with PBS-T, the cell samples were visualized under a DE/DMI6000B inverted fluorescence microscope (Leica, Wetzlar, HE, Germany).

Gene	Forward primer (5′-3′)	Reverse primer (5′-3′)
CDK5	GTACTCCACGTCCATCGACATG	GCCATTGTTCCTCAGTCGGTGT
ATG12	GAAGGCTGTAGGAGACACTCCT	GGAAGGGGCAAAGGACTGATTC
BNIP3	GCTCCAAGAGTTCTCACTGTGAC	GTTTTTCTCGCCAAAGCTGTGGC
LC3	CTGCCTGTCCTGGATAAGACCA	CTGGTTGACCAGCAGGAAGAAG
BECN1	CAGCCTCTGAAACTGGACACGA	CTCTCCTGAGTTAGCCTCTTCC
SQSTM1/p62	GCTCTTCGGAAGTCAGCAAACC	GCAGTTTCCCGACTCCATCTGT
PINK1	CGACAACATCCTTGTGGAGTGG	CATTGCCACCACGCTCTACACT
OPTN	AGGTGGAGAGACTTGAAGTCGC	TCCTCGCTGTCTGCTTCTCAGT
P21	TCGCTGTCTTGCACTCTGGTGT	CCAATCTGCGCTTGGAGTGATAG
GAPDH	CATCACTGCCACCCAGAAGACTG	ATGCCAGTGAGCTTCCCGTTCAG

Table 1. Primer sequences used in real-time quantitative polymerase chain reaction. *ATG12* autophagy-related gene 12, *BECN1* Beclin 1, *BNIP3* BCL2 interacting protein 3, *CDK5* cyclin-dependent kinase 5, *GAPDH* glyceraldehyde-3-phosphate dehydrogenase, *LC3* microtubule-associated protein light chain 3, *OPTN* optineurin, *PINK1* PTEN-induced kinase 1, *SQSTM1/p62* sequestosome 1.

	Antibody dilution	Source	Cat. no.
Primary antibody			
Phospho-tau (Ser202, Thr205) (AT8)	1:1,000	Invitrogen	MN1020
Phospho-tau (Ser422)	1:1,000	Invitrogen	44-764G
Tau	1:1,000	Invitrogen	PA5-29610
Phospho-NF-κB p65 (Ser536)	1:1,000	ABclonal	PA1294
NF-κB p65	1:1,000	Cell Signaling Technology	8242
HA tag (For GRA16)	1:1,000	Cell Signaling Technology	3724
PP2A-B55	1:1,000	Santa Cruz Biotechnology	sc-365,282
Phospho-PTEN (Ser380)	1:1,000	Santa Cruz Biotechnology	sc-377,573
PTEN	1:1,000	Santa Cruz Biotechnology	sc-7974
Phospho-GSK3β (Ser389)	1:1,000	Proteintech	14850-1-AP
GSK3β	1:1,000	Cell Signaling Technology	9315
APOE	1:1,000	Santa Cruz Biotechnology	sc-390,925
FOXO3A	1:1,000	Santa Cruz Biotechnology	sc-48,348
Caspase 3	1:1,000	Santa Cruz Biotechnology	sc-56,053
β-actin	1:1,000	Santa Cruz Biotechnology	sc-47,778
Secondary antibody			
m-IgG$_K$ BP-HRP	1:2,000	Santa Cruz Biotechnology	sc-516,102
Goat antirabbit IgG (H + L)-HRP	1:4,000	Invitrogen	32,460
Donkey antimouse IgG (H + L)-Alexa Fluor 594	1:2,000	Invitrogen	A-21,203

Table 2. Antibodies used in Immunofluorescence and Western blot analysis.

Autophagy assay

HT-22 cells were seeded into 96-well plates at 4×10^4 cells/well and incubated for 24 h at 37 °C before the autophagy assay. The cells were treated with 100 nM thrombin for 24 h at 37 °C. As a positive control, the cells were treated with 500 nM rapamycin, an autophagy inducer, for 24 h at 37 °C, washed with 1 × assay buffer, dispensed in the Microscopy Dual Detection Reagent, and then incubated for 30 min at 37 °C away from light. Thereafter, the cells were washed with 1 × assay buffer and stained with 5 μg/mL of Hoechst33342 (Sigma–Aldrich) for 5 min at room temperature in the dark. After another round of washing with 1 × assay buffer, 100 μL of 1 × assay buffer was added to the cells in each well. Autophagic fluorescence intensity was measured at a wavelength of 480 nm using Infinite® 200 PRO fluorescence microplate reader (Tecan). In addition, the fluorescence autophagic flux was visualized under a DE/DMI6000B inverted fluorescence microscope (Leica).

Cell proliferation assay

HT-22 cells were seeded into 96-well plates at 2.5×10^3 cells/well and incubated for 24 h at 37 °C before treatment with thrombin. Thereafter, the cells were exposed to 100 nM of thrombin and incubated for 0, 24, 48, 72, and 96 h. At each time point, the cells were treated with CCK-8 reagent and incubated for 1.5 h at 37 °C. Finally, the optical density was determined at a wavelength of 450 nm using the Infinite® 200 PRO microplate reader (Tecan, Männedorf, Switzerland).

Statistical analysis

All statistical analyses were conducted using GraphPad Prism 5 (GraphPad, La Jolla, CA, USA). Data are presented as mean ± standard deviation (SD). A t-test was implemented for comparisons between two groups. One-way analysis of variance (ANOVA) followed by a Bonferroni post-hoc comparison test was applied for comparisons between three groups. Two-way ANOVAs followed by Bonferroni post-hoc comparison tests were used to compare cell viability data. Statistical significance ($P < 0.05$) was designated as follows: * indicates a difference between the control group and the control + thrombin-group, † indicates a difference between the control group and the GRA16 group, and ‡ indicates a difference between the vector group and the GRA16 group.

Results

Thrombin induces Tau hyperphosphorylation and APOE expression, which are pathologically relevant targets of AD, and partially attenuates the expression of autophagy-related factors regulated by FOXO3A

Immunofluorescence staining and western blotting were performed to determine whether thrombin treatment induces tau protein hyperphosphorylation in hippocampal neuronal cells (Fig. 1A,D). During immunofluorescence staining, thrombin treatment induced a significant increase in the fluorescence expression of hyperphosphorylated tau protein (Ser202/Thr205, AT8) in HT-22 cells (Fig. 1A). We evaluated changes in p-tau (Ser202/Thr205, AT8) protein expression by measuring fluorescence intensity (as arbitrary units [AU]). The results showed p-tau (S202/T205, AT8) levels to be significantly elevated in thrombin-treated HT-22 cells (46.1 AU) compared with untreated HT-22 cells (4.63 AU) ($P < 0.05$) (Fig. 1B). Using western blotting, we

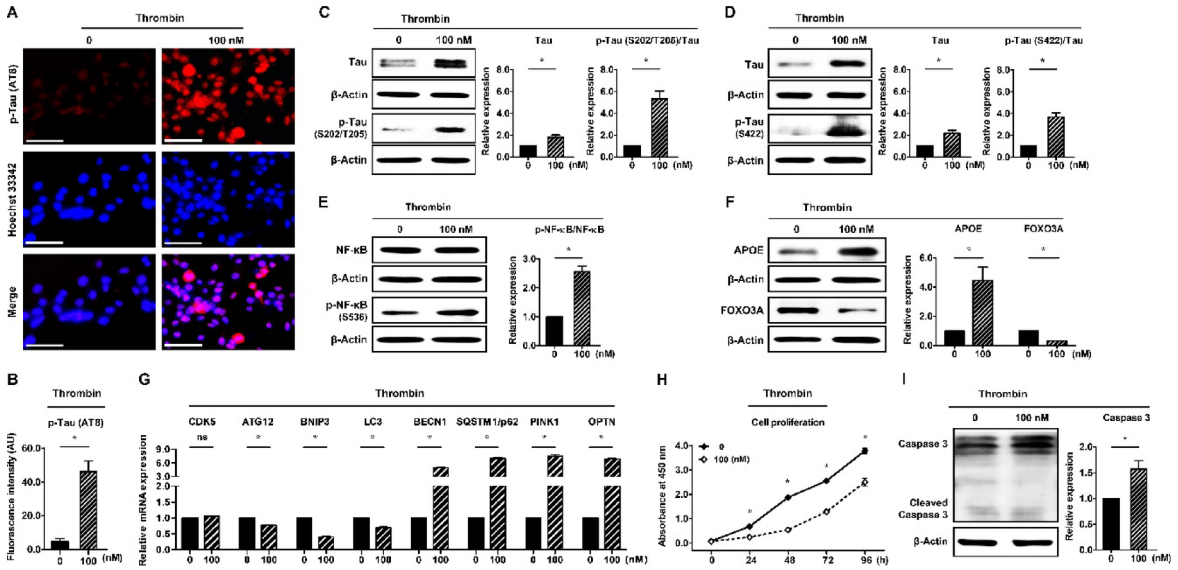

Fig. 1. Thrombin induces tau hyperphosphorylation in hippocampal neuronal cells and suppresses FOXO3A via NF-kB and APOE activation, thereby limiting the expression of autophagy-related genes. (**A**) Fluorescence analysis of phosphorylated tau (p-tau) (Ser202/Thr205) protein expression after thrombin treatment in HT-22 cells. The red areas are p-tau (Ser202/Thr205), while the blue are nuclei. Scale bar = 85 μm; (**B**) Quantification of the fluorescence intensity of p-tau (Ser202/Thr205) expression using ImageJ software; (**C**) Protein expression of tau and p-tau (Ser202/Thr205) after thrombin treatment in HT-22 cells based on Western blot analysis ($n = 3$); (**D**) Protein expression of tau and p-tau (Ser422) after thrombin treatment in HT-22 cells based on Western blot analysis ($n = 3$); (**E**) Protein expression of NF-κB and p-NF-κB (Ser536) after thrombin treatment in HT-22 cells based on western blot analysis ($n = 3$); (**F**) Protein expression of APOE and FOXO3A after thrombin treatment in HT-22 cells based on western blot analysis ($n = 3$); (**G**) Relative mRNA expression of autophagy-related factors responding to thrombin in HT-22 cells based on real-time quantitative polymerase chain reaction ($n = 5$); (**H**) Cell proliferation after thrombin treatment in HT-22 cells ($n = 5$); (**I**) Protein expression of caspase-3 after thrombin treatment in HT-22 cells based on western blot analysis ($n = 3$). * Significant at $P < 0.05$ between nontreated HT-22 cells and thrombin-treated HT-22 cells.

analyzed the total amounts of tau protein, as well as p-tau (Ser202/Thr205 and Ser422) levels. Notably, thrombin treatment increased in total tau protein and enhanced tau phosphorylation ($p < 0.05$) (Fig. 1C,D). Thereafter, to investigate the activation of NF-κB, which is known to be a major cause of tau hyperphosphorylation and tangling of hippocampal neuronal cells, NF-κB protein expression in thrombin-treated HT-22 cells was analyzed. Our results showed a significant increase in the phosphorylation of NF-κB (Ser536) ($P < 0.05$) (Fig. 1E). Meanwhile, NF-κB is a well-known inflammatory transcription factor that regulates neurodegeneration in the context of common neurodegenerative diseases. NF-κB activation increases neuroinflammation and triggers an increase in the APOE promoter function associated with AD development[24]. APOE attenuates autophagy, causing phosphorylated tau accumulation by repressing FOXO3A in the pathogenesis of AD[16]. The results of thrombin treatment, which activated NF-κB, demonstrated increased APOE protein expression and decreased FOXO3A protein expression ($P < 0.05$) (Fig. 1F). Under thrombin-induced tau hyperphosphorylation conditions, these results were characterized by a decrease in the expression of direct downstream targets of FOXO3A, such as autophagy-related gene/protein 12 (ATG12), BCL2 interacting protein 3 (BNIP3), and microtubule-associated protein light chain 3 (LC3), along with only a limited increase in certain autophagy-related genes (Beclin 1 [BECN1], sequestosome 1 [SQSTM1/p62], PTEN-induced kinase 1 [PINK1], and optineurin [OPTN]). Meanwhile, the expression of cyclin-dependent kinase 5 (CDK5), known to inhibit autophagy and induce tau hyperphosphorylation, did not show any significant difference ($P < 0.05$) (Fig. 1G). Next, to investigate the effect of thrombin on cell growth, a cell proliferation assay was analyzed over time following thrombin treatment. Reportedly, thrombin treatment reduced the rate of cell proliferation ($P < 0.05$) (Fig. 1H). In addition, the expression of caspase-3, a key mediator of apoptosis in neuronal cells, was increased in thrombin-treated HT-22 cells ($P < 0.05$) (Fig. 1I).

GRA16 affects upstream signaling pathways that modulate the Inhibition and activation of Tau hyperphosphorylation

To investigate how *T. gondii*-derived GRA16 affects tau hyperphosphorylation induced by thrombin through the regulation of PP2A and PTEN in hippocampal neuronal cells, GRA16-expressing HT-22 cells were generated using retroviral transfection. Following thrombin treatment, continuous GRA16 protein expression was confirmed by western blotting (Fig. 2A). Upon thrombin treatment, a specific increase in the expression of PP2A-B55, which dephosphorylates tau protein, was observed exclusively in GRA16-expressing HT-22 cells, accompanied by increased PTEN protein levels and enhanced dephosphorylation (Ser380) of PTEN to its active form ($P < 0.05$)

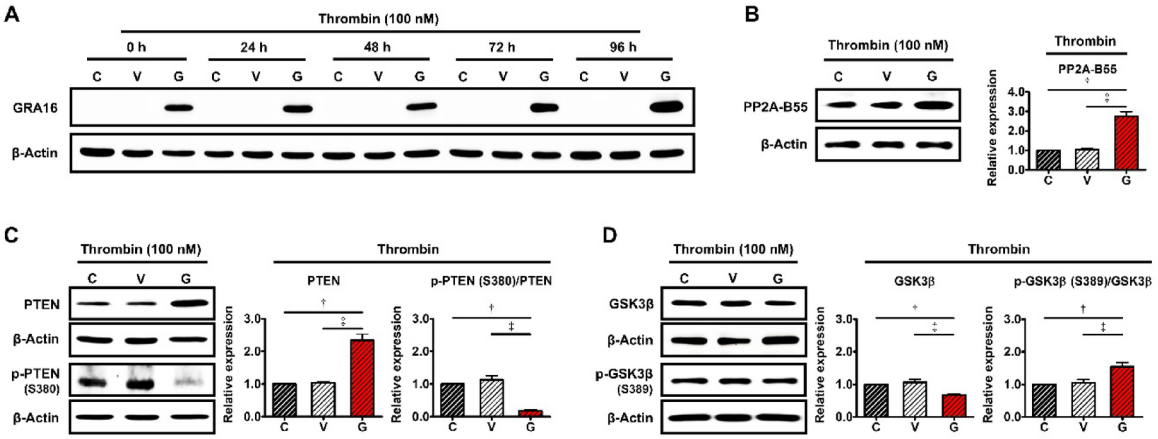

Fig. 2. GRA16 upregulated PP2A and PTEN but downregulated GSK3β in thrombin-treated HT-22 cells. (**A**) GRA16 protein expression in the experimental HT-22 cell groups (control, vector, and GRA16) after thrombin treatment based on Western blot analysis; (**B**) PP2A-B55 protein expression in the experimental HT-22 cell groups after thrombin treatment based on Western blot analysis and their relative protein expression ($n = 3$); (**C**) Western blot image of PTEN and p-PTEN (Ser380) in the experimental HT-22 cell groups after thrombin treatment and their relative protein expression ($n = 3$); (**D**) Western blot image of GSK3β and p-GSK3β (Ser389) in the experimental HT-22 cell groups after thrombin treatment and their relative protein expressions ($n = 3$). †Significant at $P < 0.05$ between the control and GRA16 in the thrombin-treated experimental HT-22 cell groups. ‡ Significant at $P < 0.05$ between the vector and GRA16 in thrombin-treated experimental HT-22 cell groups.

(Fig. 2B,C). Meanwhile, GSK3β, which acts antagonistically to PP2A and PTEN during tau phosphorylation and directly induces tau hyperphosphorylation, is a key protein involved in neurodegenerative diseases and aging. Notably, Ser389 phosphorylation indicates the inactive form of GSK3β[25]. Therefore, we also analyzed the expression of GSK3β. Notably, we found that GRA16 decreased GSK3β expression and relatively inactivated GSK3β through phosphorylation at Ser389 ($P < 0.05$) (Fig. 2D,E). As shown in Fig. 2, GRA16 upregulates PP2A and PTEN, enzymes responsible for directly dephosphorylating p-tau proteins, and inhibits GSK3β, which promotes tau phosphorylation under thrombin-induced pathological neuroinflammation conditions.

NF-κB Inhibition by GRA16 suppresses APOE and upregulates autophagy-related factors via FOXO3A increase in thrombin-induced HT-22 cells

We subsequently investigated whether GRA16 could suppress thrombin-induced activation of NF-κB/APOE signaling and enhance autophagy-related factors via FOXO3A (Fig. 3). Notably, we found that GRA16 inhibited the phosphorylation of NF-κB (Ser536) in HT-22 cells at the basal state before thrombin treatment ($P < 0.05$) (Fig. 3A). Additionally, we observed a decrease in APOE protein expression and an increase in FOXO3A protein expression ($P < 0.05$) (Fig. 3B). However, no significant difference in the expression of autophagy-related genes was noted, except for PINK1 ($P < 0.05$) (Fig. 3C). In the case of PINK1, an autophagy-inducing gene activated by PTEN, evidence suggests that the activation of PTEN by GRA16 influenced the expression of PINK1[23,26]. Meanwhile, in the thrombin-induced intracellular neuroinflammatory environment, dephosphorylation of NF-κB (Ser536) continued to occur in GRA16-expressing HT-22 cells ($P < 0.05$) (Fig. 3D). Simultaneously, the decrease in APOE protein and increase in FOXO3A protein were significantly more pronounced in the thrombin-induced neuroinflammatory state than in the basal state ($P < 0.05$) (Fig. 3E). Notably, we found a marked increase in FOXO3A protein, highlighting the substantial impact of the thrombin-induced neuroinflammatory environment in GRA16-expressing HT-22 cells. These findings also had a positive effect on autophagy-related factors. In thrombin-treated HT-22 cells expressing GRA16, all autophagy-related genes (BECN1, SQSTM1/p62, PINK1, OPTN) except CDK5, including ATG12, BNIP3, and LC3, which are directly regulated by FOXO3A, showed a more pronounced increase ($p < 0.05$) (Fig. 3F). These results confirmed that GRA16 can suppress NF-κB/APOE signaling and promote the upregulation of autophagy-related factors centered on FOXO3A under thrombin-induced neuroinflammatory conditions in HT-22 cells.

GRA16 blocks Tau hyperphosphorylation by further enhancing the thrombin-induced autophagic flux

Based on our results regarding the expression of autophagy-related signaling pathway factors regulated by GRA16, we analyzed whether GRA16 could further enhance the intracellular autophagic flux under thrombin-induced neuroinflammatory conditions and whether this could inhibit tau hyperphosphorylations in HT-22 cells (Fig. 4). Using an autophagy assay, we examined autophagic fluorescence and quantified the corresponding fluorescence intensity in HT-22 cells following thrombin treatment and observed changes in autophagic flux induced by GRA16 ($P < 0.05$) (Fig. 4A,B). Rapamycin, a well-known autophagy inducer, served as a positive control and significantly increased autophagic fluorescence (23,138 AU) ($P < 0.05$) (Fig. 4A,B). Under basal conditions (i.e., nontreated HT-22 cells), there were no significant differences in autophagic fluorescence among

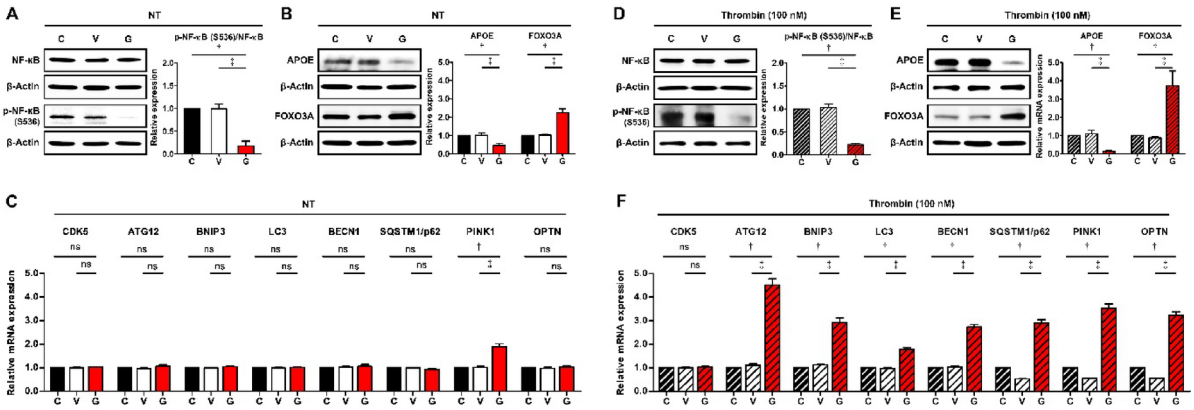

Fig. 3. GRA16 inhibited NF-κB, thereby enhancing the expression of autophagy-related factors by suppressing APOE and increasing FOXO3A in thrombin-induced cellular neuroinflammation. (**A**) Western blot images of NF-κB and p-NF-κB (Ser536) in the experimental HT-22 cell groups without thrombin ($n=3$); (**B**) Protein expressions of APOE and FOXO3A in the experimental HT-22 cell groups without thrombin based on western blot analysis ($n=3$); (**C**) Relative mRNA expressions of autophagy-related genes in the experimental HT-22 cell groups without thrombin based on real-time qPCR ($n=5$); (**D**) Western blot images of NF-κB and p-NF-κB (Ser536) in the experimental HT-22 cell groups with thrombin treatment ($n=3$); (**E**) protein expressions of APOE and FOXO3A in the experimental HT-22 cell groups with thrombin treatment based on western blot analysis ($n=3$); (**F**) relative mRNA expressions of autophagy-related genes in the experimental HT-22 cell groups with thrombin treatment based on real-time qPCR ($n=5$). †Significant at $P<0.05$ between the control and GRA16 in the experimental HT-22 cell groups without or with thrombin treatment. ‡ Significant at $P<0.05$ between the vector and GRA16 in the experimental HT-22 cell groups without or with thrombin treatment.

the control (9,883 AU), vector (10,005 AU), and GRA16 (11,090 AU) groups ($P<0.05$) (Fig. 4A,B). In contrast, following thrombin treatment, autophagic fluorescence increased in all experimental groups, with GRA16-expressing HT-22 cells displaying the highest fluorescence levels (27,273 AU) compared with the control (17,175 AU) and vector (16,769 AU) groups ($P<0.05$) (Fig. 4A,B). Next, we used fluorescence microscopy to analyze the fluorescence intensity of hyperphosphorylated tau proteins after thrombin treatment. Under basal conditions (i.e., nontreated HT-22 cells), we found no significant differences in the fluorescence intensity of phosphorylated tau (Ser202/Thr205, AT8) between the control (7.19 AU), vector (6.71 AU), and GRA16 (5.92 AU) groups ($P<0.05$) (Fig. 4C,D). In contrast, following thrombin treatment, phosphorylated tau (Ser202/Thr205, AT8) levels were markedly lower in GRA16-expressing cells (17.06 AU) compared with those in the control (50.2 AU) and vector (53.51 AU) groups ($P<0.05$) (Fig. 4E,F). We conducted a western blot analysis to assess the phosphorylation of tau proteins at two sites (Ser202/Thr205 and Ser422). Under basal conditions (i.e., nontreated HT-22 cells), there were no significant differences in phosphorylated tau (Ser202/Thr205 and Ser422) relative to total tau between any of the experimental groups ($P<0.05$) (Fig. 4G,H). Conversely, following thrombin treatment, GRA16-expressing cells exhibited a significantly greater reduction in phosphorylation at both sites (Ser202/Thr205 and Ser422) compared with the control and vector groups ($P<0.05$) (Fig. 4I,J). Next, we analyzed cell growth based on changes in autophagy under thrombin-mediated cellular tau aggregates conditions. Following thrombin treatment, GRA16-expressing HT-22 cells exhibited relatively low proliferation ($P<0.05$) (Fig. 4K), similar to that observed in control HT-22 cells treated with rapamycin. However, cell proliferation tended to gradually increase over time across all HT-22 cell groups ($P<0.05$) (Fig. 4K). We analyzed the effects of suppression of cell proliferation due to increased autophagy on cell apoptosis and cell-cycle arrest. Caspase-3 protein, a marker of cell apoptosis, including its active form did not differ significantly, either generally or in its active form (cleaved caspase-3), between the experimental groups with nontreated or thrombin-treated HT-22 cells ($P<0.05$) (Fig. 4L,M). Conversely, we found significantly elevated levels of cell-cycle arrest marker p21 in nontreated and thrombin-treated GRA16-expressing HT-22 cells ($P<0.05$) (Fig. 4O,P). Reportedly, under thrombin-induced neuroinflammatory conditions, GRA16 enhances intracellular autophagic flux, effectively reducing the accumulation of tau and concurrently slowing cell proliferation by modulating the cell-cycle to promote autophagy.

Discussion

The current study investigated the interplay between *T. gondii* GRA16, tau hyperphosphorylation and aggregation, and autophagy in hippocampal neurons experimentally induced with neurofibrillary degeneration at the cellular level. For this purpose, HT-22 cells, a murine hippocampal neuronal cell line, were treated with thrombin to induce tau hyperphosphorylation, after which the mechanisms regulating tau phosphorylation and autophagy following GRA16 transduction were analyzed.

Thrombin induces hyperphosphorylation of tau. In so doing, it can contribute to tauopathy, a condition associated with AD[27]. Tau hyperphosphorylation occurs at multiple sites along the tau protein, including

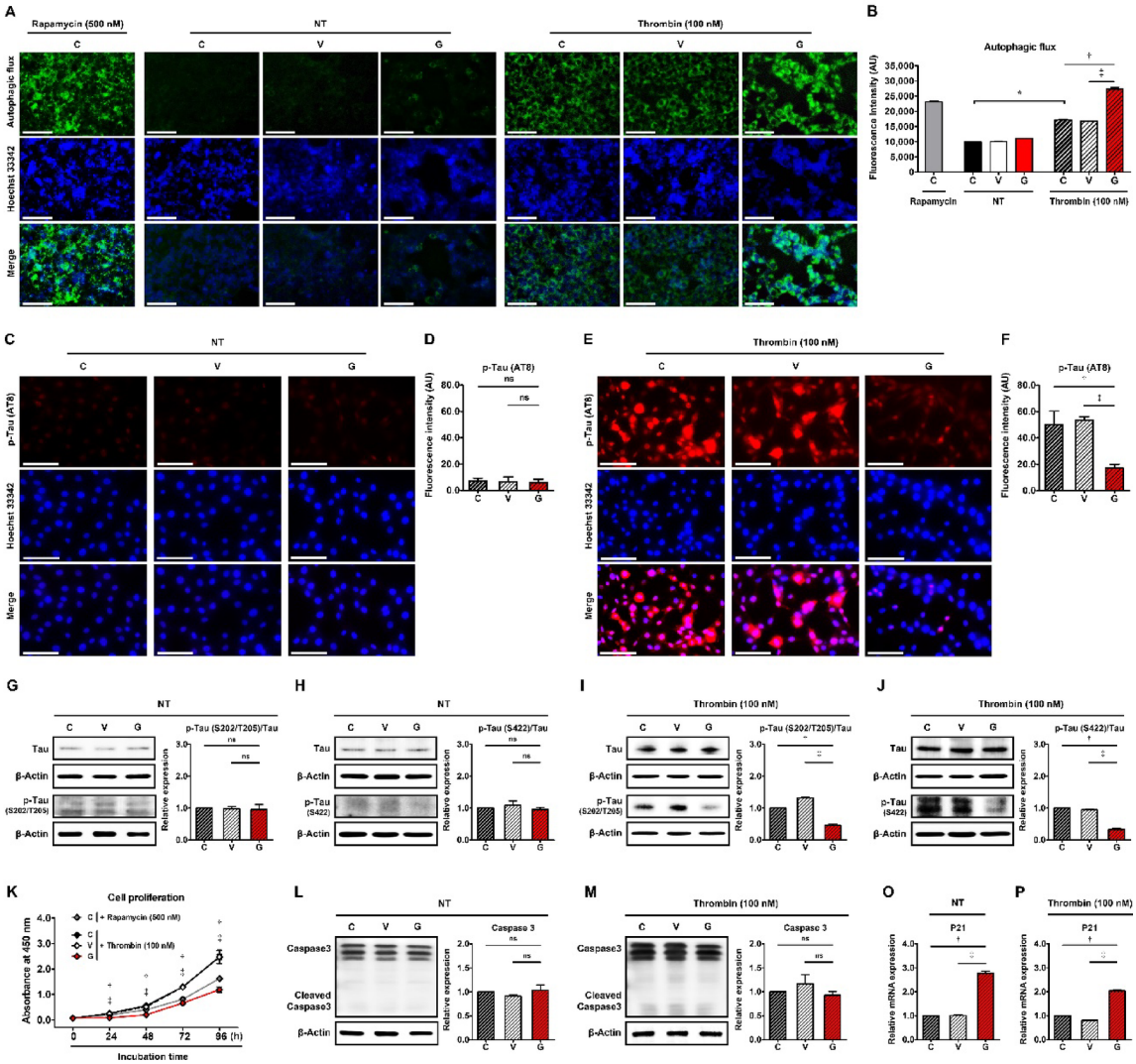

Fig. 4. GRA16 enhanced autophagy and suppressed the accumulation of hyperphosphorylated tau in thrombin-induced intracellular neurofibrillary changes. (**A**) Immunofluorescence images of autophagic flux in rapamycin-treated, nontreated (NT), and thrombin-treated experimental HT-22 cell groups. The green areas are regions of intracellular autophagic flux, while the blue areas are the nuclei. Scale bar = 75 μm; (**B**) quantification of the fluorescence intensity (AU) of autophagic flux using a fluorescence microplate reader ($n = 5$); (**C**) fluorescence images of nontreated (NT) HT-22 experimental cell groups. red indicates intracellular p-tau (Ser202/Thr205) proteins, whereas the areas stained blue are nuclei. Scale bar = 90 μm; (**D**) quantification of the AU of p-tau (Ser202/Thr205) using ImageJ ($n = 3$); (**E**) Fluorescence images of the thrombin-treated HT-22 experimental cell groups. The red areas are intracellular p-tau (Ser202/Thr205) proteins, while the blue areas are nuclei. Scale bar = 90 μm; (**F**) Quantification of the AU of p-tau (Ser202/Thr205) using ImageJ software ($n = 3$); (**G**) western blot images of tau and p-tau (Ser202/Thr205) proteins in NT HT-22 experimental cell groups ($n = 3$); (**H**) western blot images of tau and p-tau (Ser422) proteins in NT HT-22 experimental cell groups ($n = 3$); (**I**) western blot images of tau and p-tau (Ser202/Thr205) proteins in thrombin-treated HT-22 experimental cell groups ($n = 3$); (**J**) western blot images of tau and p-tau (Ser422) proteins in thrombin-treated HT-22 experimental cell groups ($n = 3$); (**K**) cell proliferation in rapamycin-treated HT-22 cells, NT experimental HT-22 cells, and thrombin-treated experimental HT-22 cells ($n = 5$); (**L**) western blot images of caspase-3 proteins in NT experimental HT-22 cells ($n = 3$); (**M**) western blot images of caspase-3 proteins in thrombin-treated experimental HT-22 cells ($n = 3$); (**O**) relative mRNA expression of p21 in the experimental HT-22 cell groups without thrombin ($n = 5$); (**P**) relative mRNA expression of p21 in the thrombin-treated experimental HT-22 cell groups ($n = 5$). *Significant at $P < 0.05$ between NT HT-22 cells and thrombin-treated HT-22 cells. †Significant at $P < 0.05$ between the control and GRA16 in the experimental HT-22 cell groups with thrombin treatment. ‡Significant at $P < 0.05$ between the vector and GRA16 in the experimental HT-22 cell groups with thrombin treatment.

Thr181 (AT270), Ser202/Thr205 (AT8), Ser214/Thr212 (AT100), Ser396/Ser404 (PHF1), and Ser422 (AP422)[28]. Herein, we selected the p-taus Ser202/Thr205 and Ser422 as marker proteins for tau hyperphosphorylation and thrombin-induced tau aggregation[7]. These two phosphorylation sites are help form NFTs in HT-22 cells following thrombin treatment. They have previously been employed in neuroinflammation research as markers in cellular models, including AD[7–9]. Meanwhile, Neddens et al. (2018) and Alonso et al. (2018) provided evidence to distinguish hyperphosphorylated tau (Ser202/Thr205 and Ser422) from regular p-tau, demonstrating that hyperphosphorylated tau exhibits a three- to four-fold increase in the number of phosphate moles per mole compared to regular p-tau[28,29]. Also, Elevated total tau (t-tau) levels in cerebrospinal fluid (CSF) are a hallmark of Alzheimer's disease (AD) and are believed to reflect ongoing neurodegeneration[30]. Therefore, based on our western blot analysis, which revealed that the relative expression of p-tau (Ser202/Thr205) increased by 5.34-fold and that of p-tau (Ser422) increased by 3.7-fold following treatment with 100 nM thrombin in HT-22 cells, we can conclude that intracellular tau hyperphosphorylation and aggregation were induced.

NF-κB, a well-established inflammatory transcription factor that drives neurodegeneration, has emerged as a significant target in inflammatory disease research owing to its broad involvement in cellular inflammatory responses[24]. APOE, which promotes neuroinflammation by reducing amyloid-β clearance and increasing phosphorylated tau accumulation in AD, is an NF-κB-dependent factor whose expression is elevated by activated NF-κB. The increase in NF-κB-dependent APOE promoter activity may attenuate autophagy by repressing FOXO3A in the pathogenesis of AD[16]. Notably, our results revealed that NF-κB and APOE were upregulated in thrombin-treated HT-22 cells, which consequently decreased FOXO3A through NF-κB-dependent APOE activation. In contrast, GRA16-expressing HT-22 cells showed an increase in PP2A-B55 expression despite thrombin treatment, whereas NF-κB and APOE levels significantly decreased. The inactivation of NF-κB-dependent APOE by GRA16 markedly increased FOXO3A expression.

FOXO3A has been associated with the transcriptional regulation of autophagy in neuronal cells. Mounting evidence indicates that FOXO3A directly activates the transcription of ATG12, BNIP3, and LC3, thereby protecting neuronal cells from the toxic effects of abnormal protein aggregation or misfolding[16]. Our results indicated that inhibiting FOXO3A in thrombin-treated HT-22 cells suppressed the expression of these genes, thereby restricting the autophagic flux. In contrast, GRA16-expressing HT-22 cells exhibited an increase in the expression of all autophagy-related genes, including FOXO3A downstream genes, thereby inducing a more pronounced induction of the autophagic flux. Meanwhile, CDK5, a serine/threonine kinase, induces tau hyperphosphorylation at multiple epitopes associated with AD[31]. Under pathological conditions such as the excessive stimulation of N-methyl-D-aspartate (NMDA) receptors, the calcium-dependent protease calpain is activated. This leads to the cleavage of p35, a CDK5 regulatory protein, and to the generation of a truncated fragment known as p25[31]. The hyperactive CDK5/p25 complex aberrantly phosphorylates multiple residual serines and threonines on the tau protein[31]. Despite the occurrence of thrombin-induced tau hyperphosphorylation, we found no significant changes in CDK5 expression in the present study. This discrepancy may be because thrombin induces tau hyperphosphorylation by activating the GSK3β pathway, which is distinct from the CDK5-mediated mechanism. However, further investigation is required to confirm this hypothesis. Previous studies have shown that PP2A-B55 and PTEN act as upstream phosphatases in the tau dephosphorylation process[32,33] and are also tumor suppressors upregulated by GRA16[21–23]. GSK3β is a direct tau-phosphorylating enzyme that is highly expressed in neurodegenerative diseases, with recent studies showing a correlation between GSK3β and activated NF-κB[25]. Our results have been the first to demonstrate that, in the context of thrombin-induced tau hyperphosphorylation and aggregation in hippocampal neuronal cells, GRA16 actively induces autophagy to facilitate the clearance of hyperphosphorylated and misfolded tau proteins and aggregates.

Rapamycin inhibits cell proliferation and induces autophagy, a cellular process responsible for removing or recycling cellular components. It is also an inhibitor of the protein kinase, mammalian target of rapamycin (mTOR)[34]. Clinically, it is widely used as an immunosuppressant[34]. Herein, rapamycin treatment simultaneously enhances autophagic flux and inhibits cell proliferation in HT-22 cells. We found similar effects in thrombin-treated GRA16-expressing cells. To investigate possible causes of the observed suppression of cell proliferation, we compared the expression levels of the cell-cycle arrest factor p21 and caspase 3 and cleaved caspase 3, which are the markers of apoptosis[35,36]. We found no significant differences between groups in the expression levels of caspase 3 and cleaved caspase 3, despite thrombin treatment. In contrast, we saw high levels of p21 expression in GRA16-expressing cells, with and without thrombin treatment. Notably, GRA16 induced high expression of PP2A-B55 and FOXO3A, which are involved in autophagy regulation and cell-cycle arrest. Therefore, GRA16 activates autophagy in response to thrombin-induced neuroinflammation. This causes the suppression of tau hyperphosphorylation and tau aggregate formation, and the attenuation of cell proliferation through the induction of cell-cycle arrest.

T. gondii is an obligate intracellular protozoan capable of invading and replicating in the cells of warm-blooded animals[37]. During host cell infection, *T. gondii* induces immune evasion mechanisms that suppress innate and adaptive immunity by releasing several secretory proteins from three types of specialized secretory organelles: micronemes, rhoptries, and dense granules[23,37]. This host signaling pathway is essential for *T. gondii* fitness, enabling its survival and proliferation within host cells[23]. Conversely, this immune evasion mechanism could serve to protect the host brain cells in the context of neurodegenerative diseases. Our previous study demonstrated that enhancing the production of anti-inflammatory cytokines in disease-related inflammatory states suppresses neuroinflammation and restores homeostasis[38,39]. These results therefore suggest the possibility that proteins secreted during *T. gondii* infection, such as GRA16, may have a mitigating effect on diseases, including AD.

In conclusion, the current study confirmed that GRA16 enhances tau dephosphorylation in tauopathies driven by tau hyperphosphorylation and promotes the clearance of tau aggregates through autophagy. Our results uncover a unique regulatory mechanism of GRA16 at the cellular level of the AD environment, with

intracellular NFTs being a pathological feature, and suggest that GRA16 could be a novel therapeutic strategy for targeting tau and autophagy.

Data availability

The datasets used and/or analysed during the current study are available from the corresponding author on reasonable request.

Received: 5 December 2024; Accepted: 28 April 2025
Published online: 20 May 2025

References

1. Ciurea, V. A. et al. Alzheimer's disease: 120 years of research and progress. *J. Med. Life*. **16**, 173–177 (2023).
2. Deture, M. A. et al. The neuropathological diagnosis of Alzheimer's disease. *Mol. Neurodegener*. **14**, 32 (2019).
3. Chen, Y. et al. Tau and neuroinflammation in Alzheimer's disease: interplay mechanisms and clinical translation. *J. Neuroinflammation*. **20**, 165 (2023).
4. Moore, K. B. E. et al. Hyperphosphorylated Tau (p-tau) and drug discovery in the context of Alzheimer's disease and related Tauopathies. *Drug Discov Today*. **28**, 103487 (2023).
5. Laurent, C. et al. Tau and neuroinflammation: what impact for Alzheimer's disease and tauopathies? *Biomed. J.* **41**, 21–33 (2018).
6. Noble, W. et al. The importance of Tau phosphorylation for neurodegenerative diseases. *Front. Neurol.* **4**, 83 (2013).
7. Suo, Z. et al. Rapid Tau aggregation and delayed hippocampal neuronal death induced by persistent thrombin signaling. *J. Biol. Chem.* **278**, 37681–37689 (2003).
8. Iannucci, J. et al. Thrombin, a key driver of pathological inflammation in the brain. *Cells* **12**, 1222 (2023).
9. Bihaqi, S. W. et al. Dabigatran reduces thrombin-induced neuroinflammation and AD markers in vitro: therapeutic relevance for Alzheimer's disease. *Cereb. Circ. - Cogn. Behav.* **2**, 100014 (2021).
10. Zhang, Z. et al. Autophagy in Alzheimer's disease pathogenesis: therapeutic potential and future perspectives. *Ageing Res. Rev.* **72**, 101464 (2021).
11. Silva, M. C. et al. Prolonged Tau clearance and stress vulnerability rescue by Pharmacological activation of autophagy in Tauopathy neurons. *Nat. Commun.* **11**, 3258 (2020).
12. Liu, X. et al. The emerging role of autophagy and mitophagy in tauopathies: from pathogenesis to translational implications in Alzheimer's disease. *Front. Aging Neurosci.* **14**, 1022821 (2022).
13. Bai, I. et al. Epigenetic regulation of autophagy in neuroinflammation and synaptic plasticity. *Front. Immunol.* **15**, 1322842 (2024).
14. Williams, T. et al. Therapeutic approaches targeting Apolipoprotein E function in Alzheimer's disease. *Mol. Neurodegener*. **15**, 1–19 (2020).
15. Maloney, B. et al. Important differences between human and mouse APOE gene promoters: limitation of mouse APOE model in studying Alzheimer's disease. *J. Neurochem*. **103**, 1237–1257 (2007).
16. Sohn, H. Y. et al. ApoE4 attenuates autophagy via FoxO3a repression in the brain. *Sci. Rep.* **11**, 17604 (2021).
17. Liu, Q. Q. et al. The role of Foxo3a in neuron-mediated cognitive impairment. *Front. Mol. Neurosci.* 17 (2024).
18. Bougdour, A. et al. Host cell subversion by Toxoplasma gra16, an exported dense granule protein that targets the host cell nucleus and alters gene expression. *Cell. Host Microbe*. **13**, 489–500 (2013).
19. Lu, X. X. et al. *PTEN* inhibits cell proliferation, promotes cell apoptosis, and induces cell cycle arrest via downregulating the PI3K/AKT/*hTERT*Pathway in lung adenocarcinoma A549 cells. *BioMed Res. Int.* **2016**, 2476842 (2016).
20. Pan, J. et al. Targeting protein phosphatases for the treatment of inflammation-related diseases: from signaling to therapy. *Signal. Transduct. Target. Ther.* **7**, 177 (2022).
21. Kim, S. G. et al. Increase in the nuclear localization of PTEN by the *Toxoplasma* GRA16 protein and subsequent induction of p53-dependent apoptosis and anticancer effect. *J. Cell. Mol. Med.* **23**, 3234–3245 (2019).
22. Seo, S. H. et al. *Toxoplasma* GRA16 inhibits NF-κB activation through PP2A-B55 upregulation in Non-Small-Cell lung carcinoma cells. *Int. J. Mol. Sci.* **21**, 6642 (2020).
23. Seo, S. H. et al. PTEN/AKT signaling pathway related to hTERT downregulation and telomere shortening induced in *Toxoplasma* GRA16-expressing colorectal cancer cells. *Biomed. Pharmacother*. **153**, 113366 (2022).
24. Sun, E. et al. The pivotal role of NF-kB in the pathogenesis and therapeutics of Alzheimer's disease. *Int. J. Mol. Sci.* **23**, 8972 (2022).
25. Calvo, B. et al. GSK3β Inhibition by phosphorylation at Ser389 controls neuroinflammation. *Int. J. Mol. Sci.* **24**, 337 (2022).
26. Han, Y. et al. Roles of PINK1 in regulation of systemic growth Inhibition induced by mutations of PTEN in Drosophila. *Cell. Rep.* **34**, 108875 (2021).
27. Toral-Rios, D. et al. GSK3β and Tau protein in Alzheimer's disease and epilepsy. *Front. Cell. Neurosci.* **14**, 19 (2020).
28. Neddens, J. et al. Phosphorylation of different Tau sites during progression of Alzheimer's disease. *Acta Neuropathol. Commun.* **6**, 52 (2018).
29. Alonso, A. D. et al. Hyperphosphorylation of Tau associates with changes in its function beyond microtubule stability. *Front. Cell. Neurosci.* **12**, 338 (2018).
30. Visser, P. J. et al. Cerebrospinal fluid Tau levels are associated with abnormal neuronal plasticity markers in Alzheimer's disease. *Mol. Neurodegener*. **17**, 27 (2022).
31. Pao, P. C. et al. Three decades of Cdk5. *J. Biomed. Sci.* **28**, 79 (2021).
32. Xu, Y. et al. Structure of a protein phosphatase 2A holoenzyme: insights into B55-mediated Tau dephosphorylation. *Mol. Cell.* **31**, 873–885 (2008).
33. Zhang, X. et al. Tumor suppressor PTEN affects Tau phosphorylation, aggregation, and binding to microtubules. *FASEB J.* **20**, 1272–1274 (2006).
34. Lin, X. et al. Rapamycin inhibits proliferation and induces autophagy in human neuroblastoma cells. *Biosci. Rep.* **38**, BSR20181822 (2018).
35. D'Amelio, M. et al. Caspase-3 in the central nervous system: beyond apoptosis. *Trends Neurosci.* **35**, 700–709 (2012).
36. Engeland, K. Cell cycle regulation: p53-p21-RB signaling. *Cell. Death Differ.* **29**, 946–960 (2022).
37. Seo, S. H. et al. *Toxoplasma gondii* IST suppresses inflammatory and apoptotic responses by inhibiting STAT1-mediated signaling in IFN-γ/TNF-α-stimulated hepatocytes. *Parasites Hosts Dis.* **62**, 30–41 (2024).
38. Ham, D. W. et al. Chronic *Toxoplasma gondii* infection alleviates experimental autoimmune encephalomyelitis by the immune regulation inducing reduction in IL-17A/Th17 via upregulation of SOCS3. *Neurother* **18**, 430–447 (2021).
39. Shin, J. H. et al. Reduction of amyloid burden by proliferated homeostatic microglia in *Toxoplasma gondii*-infected Alzheimer's disease model mice. *Int. J. Mol. Sci.* **22**, 2764 (2021).

Author contributions

(Conceptualization) S.H.S. and E.H.S; (Material preparation and methodology) S.H.S. and J.E.L; (Data collec-

tion and analysis) S.H.S, D.W.H, and J.E.L.; (Project administration and supervision) E.H.S.; (first draft of the manuscript) S.H.S. and E.H.S.; All authors reviewed the manuscript.

Funding
This work was supported by the National Research Foundation of Korea (NRF) grant funded by the Korean government (MSIT) (No. NRF-2022R1A2C1009234) and by grant no. 14-2023-0005 from the Seoul National University Bundang Hospital (SNUBH) Research Fund.

Declarations

Competing interests
The authors declare no competing interests.

Additional information
Supplementary Information The online version contains supplementary material available at https://doi.org/10.1038/s41598-025-00271-4.

Correspondence and requests for materials should be addressed to E.-H.S.

Reprints and permissions information is available at www.nature.com/reprints.

Publisher's note Springer Nature remains neutral with regard to jurisdictional claims in published maps and institutional affiliations.